

REPORT DOCUMENTATION PAGE			Form Approved OMB No. 0704-0188	
Public reporting burden for this collection of information is estimated to average 1 hour per response, including the time for reviewing instructions, searching existing data sources, gathering and maintaining the data needed, and completing and reviewing this collection of information. Send comments regarding this burden estimate or any other aspect of this collection of information, including suggestions for reducing this burden to Department of Defense, Washington Headquarters Services, Directorate for Information Operations and Reports (0704-0188), 1215 Jefferson Davis Highway, Suite 1204, Arlington, VA 22202-4302. Respondents should be aware that notwithstanding any other provision of law, no person shall be subject to any penalty for failing to comply with a collection of information if it does not display a currently valid OMB control number. <b>PLEASE DO NOT RETURN YOUR FORM TO THE ABOVE ADDRESS.</b>				
1. REPORT DATE (DD-MM-YYYY) 2014		2. REPORT TYPE Open Literature		3. DATES COVERED (From - To)
4. TITLE AND SUBTITLE Biophysical aspects of cyclodextrin interaction with paraoxon		5a. CONTRACT NUMBER		
		5b. GRANT NUMBER		
		5c. PROGRAM ELEMENT NUMBER		
6. AUTHOR(S) Soni, S-D, Bhonsle, JB, Garcia, GE		5d. PROJECT NUMBER		
		5e. TASK NUMBER		
		5f. WORK UNIT NUMBER		
7. PERFORMING ORGANIZATION NAME(S) AND ADDRESS(ES)  US Army Medical Research Institute of Chemical Defense ATTN: MCMR-CDR-I 3100 Ricketts Point Road		8. PERFORMING ORGANIZATION REPORT NUMBER  USAMRICD-P13-018		
9. SPONSORING / MONITORING AGENCY NAME(S) AND ADDRESS(ES) Defense Threat Reduction Agency 8725 John J. Kingman Road STOP 6201 Fort Belvoir, VA 22060-6201		10. SPONSOR/MONITOR'S ACRONYM(S)		
		11. SPONSOR/MONITOR'S REPORT NUMBER(S)		
12. DISTRIBUTION / AVAILABILITY STATEMENT  Approved for public release; distribution unlimited				
13. SUPPLEMENTARY NOTES Published in Magnetic Resonance in Chemistry, 52(3), 111-114, 2014. This research was supported by the Defense Threat Reduction Agency – Joint Science and Technology Office, Medical S&T Division project # CBM. SCAV.01.10.WR.001.				
14. ABSTRACT See reprint.				
15. SUBJECT TERMS NMR; cyclodextrins; paraoxon; organophosphate oxon; pesticide; 1H; molecular model; Jobs plot; Benesi–Hildebrand plot				
16. SECURITY CLASSIFICATION OF:			17. LIMITATION OF ABSTRACT  UNLIMITED	18. NUMBER OF PAGES  4
a. REPORT UNCLASSIFIED	b. ABSTRACT UNCLASSIFIED	c. THIS PAGE UNCLASSIFIED		
			19a. NAME OF RESPONSIBLE PERSON Gregory E. Garcia	
			19b. TELEPHONE NUMBER (include area code) 410-436-6009	

# Biophysical aspects of cyclodextrin interaction with paraoxon

Sunil-Datta Soni,<sup>a</sup> Jayendra B. Bhonsle<sup>b</sup> and Gregory E. Garcia<sup>b\*</sup>

Cyclodextrins are torus-shaped polymers of glucose that can bind organophosphorous compounds such as nerve agents and pesticides. We demonstrate here that cyclodextrin can bind up to two paraoxon molecules with a  $K_{av}$  of  $6775\text{ M}^{-1}$ . Molecular modeling shows that the paraoxon appears to bind in polar opposite orientation and have an average binding energy of  $-89\text{ Kcal/mol}$ . Published 2013. This article is a U.S. Government work and is in the public domain in the USA.

**Keywords:** NMR; cyclodextrins; paraoxon; organophosphate oxon; pesticide;  $^1\text{H}$ ; molecular model; Jobs plot; Benesi–Hildebrand plot

## Introduction

Because of the initial discovery that cyclodextrins (CDs) can bind and catalyze the hydrolysis of organophosphorus (OP) pesticides and nerve agents,<sup>[1–3]</sup> these compounds have been of interest as potential scavengers of OPs. The intrinsic ability of CDs to hydrolyze OPs has been improved by several modifications such as capping on the primary rim and addition of nucleophile adducts on the secondary rim.<sup>[4,5]</sup> To make improvements in CD design and gain insights into the structural relationships to OP-scavenging activity, we began by examining the interactions of  $\beta$ -CDs with paraoxon (PX) by NMR techniques and molecular modeling. Whereas NMR techniques have been used to evaluate the interactions of CDs with other molecules, as far as we know, this is the first report on the interaction of CDs with this pesticide using this technique.

## Materials and Methods

The  $\beta$ -CD and paraoxon were purchased from Sigma Aldrich, Saint Louis, MO, and used without further purification; purity was checked using proton NMR and was taken into account in the calculations. The  $\beta$ -CD was 98% pure as supplied, and the water content was 15%. All compounds were dissolved in 99.8%  $\text{D}_2\text{O}$ . The NMR experiments were performed on Varian's Unity Inova at 600 MHz using a 5-mm Penta PFG probe at 25 °C. Either internal 4,4-Dimethyl-4-Silapentane-1-Sulfonic acid (DSS) or

**Table 1.** Chemical shift values (ppm) of  $\beta$ -cyclodextrin and paraoxon at 25 °C

Compound	Resonance	Chemical shift (ppm)	
		Without complexation	1 : 1 complex
$\beta$ -CD	H1'	4.938	4.956
	H2'	3.516	3.536
	H3'	3.834	3.839
	H4'	3.454	3.475
	H5'	3.733	3.726
	H6', 6"	3.750	3.764
Paraoxon	$\text{CH}_3$ (triplet)	1.361	1.250
	$\text{CH}_2$ (multi)	4.332	4.226
	H3,5 (doublet)	7.445	7.350
	H2,6 (doublet)	8.334	8.226

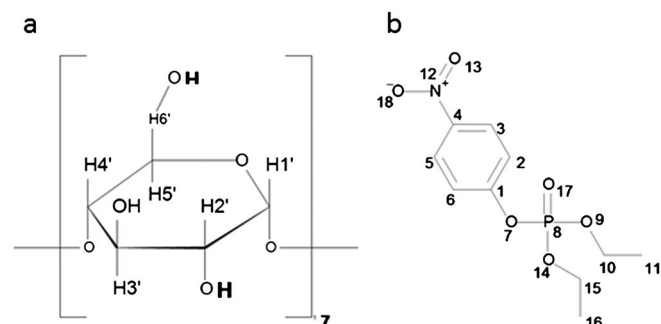


**Figure 1.** Compound structures. a.  $\beta$ -cyclodextrin; b. paraoxon. The number schemes are shown for the compounds.

residual Deuterium hydroxide (HOD) peak was used as proton reference. A standard (s2pul) pulse sequence was used and 90° pulse calibrated on the sample with a 3 s relaxation delay. A total of 32 scans were collected for each data set. Data were processed using MestReNova software (Mestrelab Research, Spain) with 1 Hz line broadening and zero filling to 32 K. In case of multiplets, the average chemical shifts in parts per million are reported. All proton assignments were confirmed using 2D data set (COSY and TOCSY).  $\beta$ -CD and PX were mixed and equilibrated to 25 °C before proton NMR data were collected and chemical shifts were extracted. The structure of PX was built and minimized with MMFF force field and charges. The molecular volume and molecular Van-der-Waals surface area (measured in cubic Angstroms and square Angstrom) were determined. The crystal structure of  $\beta$ -CD (PDB ID=1DMB) was downloaded (Protein Data bank [www.pdb.org](http://www.pdb.org)) and cleaned as follows. The  $\beta$ -CD ligand was extracted from 1DMB and minimized with MMFF force field and charges. This

\* Correspondence to: Gregory E. Garcia, Physiology and Immunology, USAMRICD, Aberdeen Proving Ground, MD, USA. E-mail: [gregory.e.garcia.civ@mail.mil](mailto:gregory.e.garcia.civ@mail.mil)

a Physiology and Immunology, USAMRICD, Aberdeen Proving Ground, MD, USA

b Astha Drug Discovery & Research, 5284 Randolph Rd #262, Rockville, MD, USA

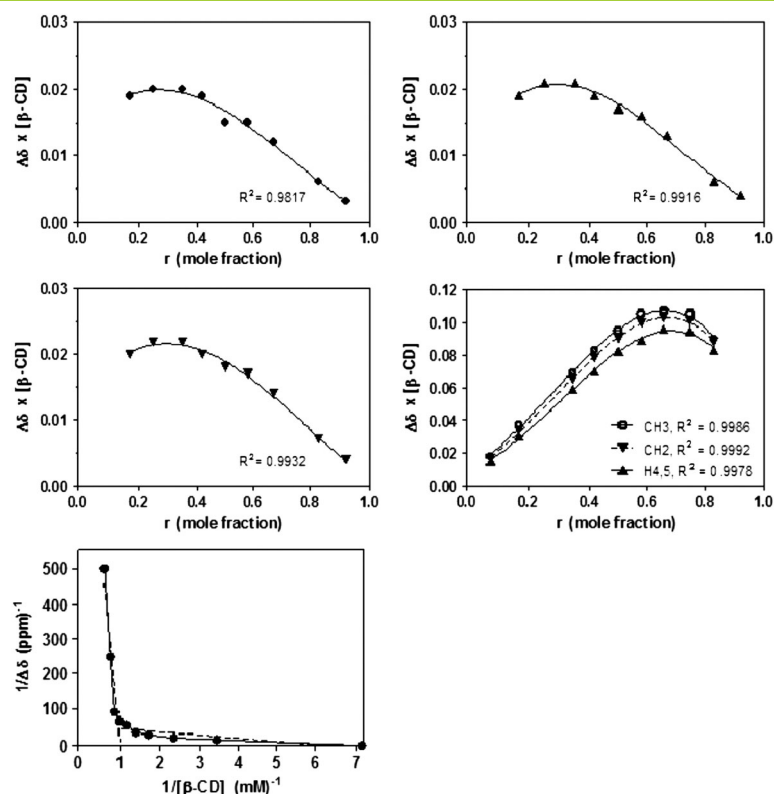


**Figure 2.** NMR analysis of paraoxon (PX) and  $\beta$ -CD interaction. Job's plot analysis (continuous variation method) was performed for  $\beta$ -CD H1', H2', and H4' protons and is shown in a–c respectively. The PX CH3, CH2, H3,5, and H2,6 plots are shown in d.  $\delta = \delta(\text{complex}) - \delta(\text{free})$ , and the Mole fraction  $r = [\text{CD}] / ([\text{CD}] + [\text{OP}])$  where CD =  $\beta$ -CD and OP = PX. The Benesi–Hildebrand plot for PX2-CD is shown in e. All concentrations are in millimolar.

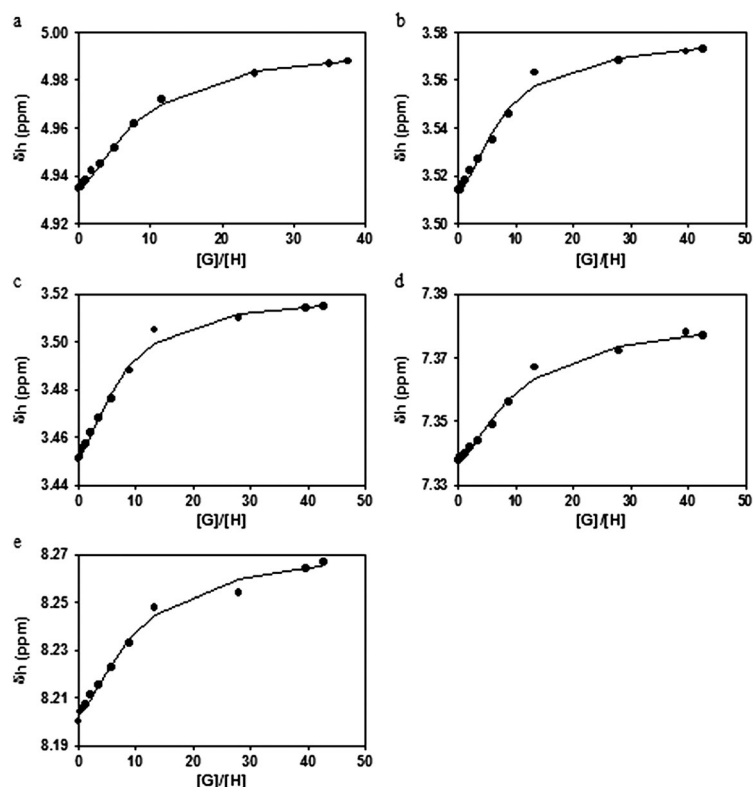


**Figure 3.** Plots of the change of chemical shift association constant generated from titration data between  $\beta$ -cyclodextrin and paraoxon. The plots show observed and calculated data for the  $\beta$ -cyclodextrin sugar resonances analyzed using nonlinear regression analysis for a. H1', b. H2', c. H5', d. H2 H8, and e. H3 H5.

was used for the docking employing the FlexiDock algorithm on the basis of genetic algorithm as implemented in Tripos SYBYL-X Version 1.3 molecular modeling software.

## Results and Discussion

The structures of  $\beta$ -CD and PX are shown in Fig. 1. The chemical shifts (ppm) for the hosts ( $\beta$ -CD), guests (PX), and 1:1 complex are reported in Table 1. The NMR PX/CD data were compiled to generate values to the Job's plots shown in Fig. 2. The continuous variation method [(H) + (G) = (constant)] of Job's plots are shown in Fig. 2a–d. The  $\Delta\delta$  chemical shifts of  $\beta$ -CD H1', H2', and H4' are shown in Fig. 2a–c and those of PX, CH<sub>3</sub>, CH<sub>2</sub>, H<sub>2</sub>,<sup>5</sup> and H<sub>3</sub>,<sup>6</sup> are shown in Fig. 2d. The  $\beta$ -CD plots yield maxima of 0.33, and the PX plots yield maxima of 0.66, indicating that more than one PX molecule is binding to each CD, as typically a 1:1 ratio would yield a maximum of 0.5. Additional analysis by Benesi–Hildebrand (B–H) plot is shown in Fig. 2e. This plot did not yield a straight line, further indicating that multiple PX molecules are binding to each CD, because a simple 1:1 complex of CD and PX would yield a straight line from which the association constant  $K_{av}$  would be the slope. Thus, in our case, the association constant was determined as described by Hirose<sup>[6]</sup> where H was the host ( $\beta$ -CD) and G was the guest (PX). The  $\delta_H$  data were plotted against [G]/[H] to yield the plots shown in Fig. 3. The calculated average association constants were derived from the graphs of Fig. 3. The observed and calculated chemical shift values from nonlinear regression analysis were subject to statistical analysis using SolvStat<sup>[7]</sup> and are reported in Table 2. Because of severe overlap of some of the  $\beta$ -CD proton resonances, only some of the values are reported. The average association constant ( $K_{av}$ ) is 6557 M<sup>−1</sup> with an average standard deviation of 1118 and mean R<sup>2</sup> of 0.9932. We then examined  $\beta$ -CD accommodation of PX by molecular modeling. The computed molecular volume and molecular Van-der-Waals surface area for PX were found to be 779.56 Å<sup>3</sup> and 495.14 Å<sup>2</sup>, respectively. The computational modeling of PX into the  $\beta$ -CD cavity is shown in Fig. 4. The computational fitting of a single PX into the  $\beta$ -CD cavity is depicted in Fig. 4a and b showing the wire rendering of the primary face view and

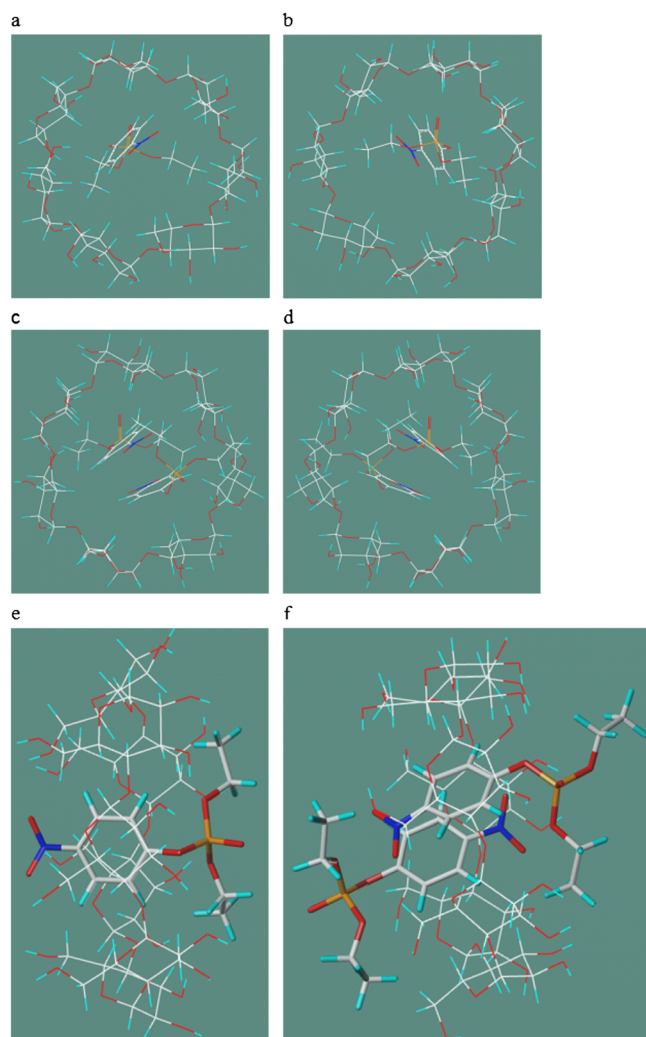


**Figure 4.** Molecular models of single and double paraoxons (PXs) within  $\beta$ -CD. Wire figures of single PX binding are shown in a (primary face) and b (secondary face). The wire figures of double PX binding are shown in c (primary face) and d (secondary face). The lateral views of single e and double f PX binding are shown with the primary face on the left and PX rendered as capped sticks. Oxygen is rendered in red, phosphorus in orange, and nitrogen in blue.

**Table 2.** Results from the nonlinear regression fit of H1', H2', H5', and H2 H8 and H3 H5 shown in Fig. 3 as association constant and with statistical errors

Proton	Parameters	$\delta_H$	$\delta_{GHG-complex}$	$K_{av}^1$ M
H1'	Values	4.9359	5.0072	6659
	SDs	0.0005	0.0023	675
	R <sup>2</sup> , SE(y)	0.9981	0.001	—
H2'	Values	3.5146	3.5873	7866
	SDs	0.0011	0.0033	1384
	R <sup>2</sup> , SE(y)	0.9930	0.0023	—
H5'	Values	3.4528	3.5278	9276
	SDs	0.0012	0.0031	1592
	R <sup>2</sup> , SE(y)	0.9930	0.0024	—
H3, H5	Values	8.2038	8.2885	4971
	SDs	0.0013	0.0062	1117
	R <sup>2</sup> , SE(y)	0.9905	0.0028	—
H2, H8	Values	7.3385	7.3916	5013
	SDs	0.0008	0.0035	1029
	R <sup>2</sup> , SE(y)	0.9921	0.0016	—
			Mean $K_{av}$	6757

secondary face views. The docking of two PX molecules into the  $\beta$ -CD cavity in the wire rendering form is shown in Fig. 4c and d for the primary and secondary face views. The docking energy of the two PX in the PX<sub>2</sub>/CD is −89 Kcal/mol, while for one PX in PX/CD, it is −55 Kcal/mol. In the lateral face views shown in Fig. 4e and f, the PX and 2PX molecules are shown as Stick renderings to highlight them vis-à-vis the  $\beta$ -CD molecules. The model shows that the phosphate and nitro portions of the PX molecule protrude out of the  $\beta$ -CD cavity. For 2PX binding, the phosphate and nitro of the second PX are polar opposite the other PX. This arrangement would allow the aligning of the phenyl portions that may produce  $\pi$ – $\pi$  interactions that enhance the docking energy for the second PX, although this would not explain the large difference in docking energies as yet other unidentified interactions could contribute.

## Acknowledgements

The authors are thankful to Mr Richard Sweeney for insightful discussion and Ms Deborah Doctor for technical support. The

views expressed are those of the author(s) and do not reflect the official policy of the Department of Army, Department of Defense, or the US Government. This research was supported by the Defense Threat Reduction Agency – Joint Science and Technology Office, Medical S&T Division project # CBM. SCAV.01.10.WR.001.

## References

- [1] C. Van Hooijdonk, J. C. A. E. Breebaart-Hansen. *Recl. Trav. Chim. Pays-Bas*. **1970**, 89, 289–299.
- [2] C. Van Hooijdonk, C. C. Groos. *Recl. Trav. Chim. Pays-Bas*. **1970**, 89, 845–856.
- [3] B. Desire, S. Saint-Andre. *Fund. Appl. Toxicol.* **1986**, 7, 646–657.
- [4] H. H. Seltzman, final report to USAMRDC on Contract No.DAMD17-94-C-4012, **1999**.
- [5] R. K. Kalakuntla, T. Wille, R. Le Provost, S. Letort, G. Reiter, S. Muller, H. Thiermann, F. Worek, G. Gouhier, O. Lafont, F. Estour. *Toxicol. Letts.* **2013**, 216, 200–205.
- [6] K. Hirose, Quantitative Analysis Of Binding Properties, in *Analytical Methods in Supramolecular Chemistry*, vol. 1 (Ed: C. A. Schalley), Wiley-VCH, Germany, **2012**, pp. 27–65.
- [7] E. J. Billo, *EXCEL for Scientists and Engineers – numerical methods*, Wiley-Interscience, John Wiley & Sons, Inc., New Jersey, **2007**, pp. 328–329.